

35 Introduction

36 Although the field of viral metagenomics is exponentially expanding the repertoire of viral
37 genome sequences available for evolutionary studies (Roossinck, 2016), it only provides a picture of
38 viral diversity over a very short geological time scale. However, viruses can leave molecular records in
39 the genomes of their hosts in the form of endogenous viral elements (EVEs). EVEs are viral sequences
40 that have transferred into the nuclear genomes of their hosts by either active or passive integration
41 mechanisms and retained over extended periods of time, sometimes millions of years. The study of
42 EVEs does allow the evolution of viruses to be traced, much like a fossil record (Aiewsakun and
43 Katzourakis, 2015). For example, the study of endogenous retroviruses has led to the conclusion that
44 retroviruses have a marine origin and that they developed in parallel with their vertebrate hosts
45 more than 450 million years ago (MYA; (Aiewsakun and Katzourakis, 2017)).

46
47 Plant EVEs were first discovered a little more than 20 years ago (Bejarano et al., 1996) and
48 have only received a fraction of the research attention directed towards endogenous retroviruses in
49 humans and animals. Most characterized plant EVEs are derivatives of viruses in the family
50 *Caulimoviridae* (Teycheney and Geering, 2011). The *Caulimoviridae* is one of the four families of
51 reverse-transcribing viruses or virus-like retrotransposons that occur in eukaryotes, and is the only
52 family of viruses with a double-stranded DNA genome that infects plants
53 (<https://talk.ictvonline.org/>). Eight different genera of the *Caulimoviridae* are currently recognized by
54 the International Committee for the Taxonomy of Viruses (ICTV), of which five (petu-, badna-,
55 caulimo-, solendo- and soymovirus) have EVE counterparts in at least one plant genome (Teycheney
56 and Geering, 2011) (Mushegian and Elena, 2015). Recently, (Geering et al., 2014) showed that EVEs
57 from an additional tentative genus of the *Caulimoviridae*, called 'Florendovirus', are widespread in
58 the genomes of cultivated and wild angiosperms and provided evidence for the oldest EVE
59 integration event yet reported in plants, at 1.8 MYA (Geering et al., 2014). Although no extant
60 florendoviruses has been identified, their endogenous fossils account for almost half of all recognized
61 *Caulimoviridae*, illustrating that fossil viral species characterized from EVEs may outnumber extant
62 ones and that they have the potential to help refine viral taxonomy. The discovery of endogenous
63 florendoviruses in ANITA grade plant species also showed that beyond mesangiosperms,
64 *Caulimoviridae* host range spans or once spanned in more basal angiosperms. Furthermore, contrary
65 to extant viral retroelements, endogenous florendovirus genomes revealed a bipartite genome
66 organization (Geering et al., 2014). These findings demonstrate that analyzing the genetic footprints
67 left by viruses in plant genomes can contribute to a better understanding of the long-term processes
68 driving the evolution of the *Caulimoviridae*.

69
70 In this study, we report on the discovery of EVEs from several novel viruses in a significant
71 number of plant genomes and we propose to create nine new virus genera in the *Caulimoviridae* to
72 accommodate these new viral species. We show that the *Caulimoviridae* host range extends to the
73 Euphyllopyte and Lycopodiophytes clades, surpassing that of any plant virus family. By analyzing the
74 distribution of different genera of the *Caulimoviridae* within different plant species, we unveil a
75 complex pattern of associations and propose a scenario in which *Caulimoviridae* would have
76 emerged together with early land plants approximately 420 million years ago and evolved principally
77 through vertical transmission.

78

79 Results

80 **Augmenting the diversity of endogenous caulimovirids**

81 The reverse transcriptase (RT) domain is the most conserved domain in the genome of viral
82 retroelements and is used for classification (Xiong and Eickbush, 1990) (Hansen and Heslop-Harrison,
83 2004). The strong sequence conservation of this domain allows high quality alignments to be
84 generated, even for distantly related taxa. We have thus used a collection of RT domains from known
85 exogenous and endogenous caulimovirids to search for related sequences across the breadth of the
86 Viridiplantae (four green algae, two basal land plants, four gymnosperms, and 62 angiosperms;
87 Supplementary Table 1) using BLAST.

88
89 Initially, over 8,400 protein-coding sequences were retrieved, all containing an RT domain with a best
90 reciprocal hit against members of the *Caulimoviridae*, as opposed to the closely related *Metaviridae*
91 (Ty3-gypsy group LTR retrotransposons). To provide a preliminary classification, sequences with at
92 least 55% amino acid identity to each other were clustered and then iteratively added to our
93 reference set of RT domains to build a phylogenetic network. The successive networks were
94 examined manually and representative sequences from each cluster were kept only when creating
95 substantially divergent branches so as to cover an extended diversity of caulimovirid RT with a core
96 sequence assortment. While this network-based approach cannot be taken as phylogenetic
97 reconstruction, it provided a practical method to explore diversity.

98
99 In the final phylogenetic network (Figure 1), 17 groups were identified, hereafter referred to as
100 operational taxonomic units (OTUs). Remarkably, nine of these OTUs lacked recognized members of
101 the *Caulimoviridae*. Four of these novel OTUs were exclusively composed of sequences from
102 gymnosperms, thereby representing a new and significant host range extension for the
103 *Caulimoviridae*. These OTUs were named Gymnendovirus 1 to 4. Two other novel OTUs were
104 composed of RTs from various angiosperms and were named Xendovirus and Yendovirus. The last
105 three novel OTUs were small in size, comprising sequences from one or two plant species (*Petunia*
106 *inflata* and *Petunia axillaris*; *Vitis vinifera*; *Glycine max*; named species-wise: Petunia-, Vitis-, and
107 Glycine-endovirus). This initial search therefore enabled uncovering a significantly augmented
108 diversity of caulimovirid RTs.

109 110 **Endogenous caulimovirid RT (ECRT) density across the Viridiplantae**

111 Using the sequences from the final phylogenetic network (Figure 1) to perform a second, more
112 comprehensive search for ECRTs in our collection of plant genomes, we detected 14,895 genomic loci
113 representing high-confidence ECRT candidates. Remarkably, ECRTs were found in nearly all seed
114 plants, ranging from gymnosperms (ginkgo and conifers) to angiosperms. However, none were
115 detected in green algae and non-seed basal land plants for which complete genomes are publicly
116 available (Supplementary Table 1). Quantitatively, over one-thousand ECRTs were detected in the
117 genome assemblies of the gymnosperms *Picea glauca* (white spruce) and *Pinus taeda* (loblolly pine),
118 as well as from the solanaceous species *Capsicum annuum* (bell pepper) (Figure 2A). In general, we
119 observed a positive correlation between plant genome size and the number of ECRTs, although there
120 were notable exceptions such as the monocot *Zea mays* (maize), which has a relatively large genome
121 at 2.1 Gb but no detectable ECRT. Five other seed plants from our sample also lacked ECRTs,
122 including two other monocots (*Zostera marina* and *Oryza brachyantha*) and three dicots in the order
123 *Brassicales* (*Arabidopsis thaliana*, *Schrenkiella parvula* and *Carica papaya*). When the number of

124 ECRTs was normalized against genome size, *Citrus sinensis* (sweet orange) and *Ricinus communis*
125 (castor bean) had the highest densities at 2.3 and 2 ECRTs per Mb, respectively (Figure 2B). The
126 ANITA grade angiosperm *Amborella trichopoda* also had a relatively high density of ECRTs (1 ECRT
127 per Mb) compared to an average density of 0.2 ECRT per Mb across the 62 seed plant species that
128 were examined.

129

130 **Caulimovirid sequences are also detected in ferns and a clubmoss**

131 As ECRTs were detected in gymnosperm genomes, we extended our search to the genomes of ferns
132 (class Polypodiopsida, basal seed plants), which represent an intermediate bifurcation in the
133 evolution of the Viridiplantae but for which no complete genome is publicly available. We retrieved
134 genomic contigs from six fern genomes that have recently been sequenced at low coverage
135 (approximately 0.4 to 2 x genome size equivalent (Wolf et al., 2015)) and screened this data set for
136 the presence of ECRTs. A total of twenty-one protein-coding ECRTs were detected in genomic contigs
137 from five out of the six fern species examined (Supplementary Table 1). Phylogenetic network
138 reconstruction using representative fern ECRTs revealed that they form two novel OTUs that were
139 named Fernendovirus 1 and 2 (Supplementary Figure 2).

140

141 To further explore the association of *Caulimoviridae* with species from basal lineages of the
142 Viridiplantae, 1,000 plant transcriptomes generated by the 1KP initiative (Matasci et al., 2014)
143 (Wickett et al., 2014) were interrogated. From this sample, we found two transcript contigs (2.4 and
144 2.8 kilobases long, respectively) in *Botrypus virginianus* (identifier BEGM-2004510) and *Lindsaea*
145 *linearis* (identifier NOKI-2097008), which contained ECRTs. Remarkably, we identified one more
146 transcript contig (identified as ENQF-2084799, 2kb) that contained an ECRT in the clubmoss
147 *Lycopodium annotinum*, which belongs to *Lycopoda*, the most basal radiation of vascular plants
148 (Tracheophyta).

149

150 **Phylogenetic reconstruction**

151 Complete or near complete viral genomes were reconstructed from each novel OTU except
152 Fernendovirus (Supplementary file 1). From the fern genomic data sets, we were able to reconstruct
153 fragments of Fernendovirus 1 & 2 genomes that contain genome coverage for phylogenetic analysis.
154 We also used the complete genomes of type species of the eight currently recognized genera in the
155 family *Caulimoviridae* (*Badnavirus*, *Caulimovirus*, *Cavemovirus*, *Petuvirus*, *Rosadnavirus*, *Solendovirus*,
156 *Soymovirus*, *Tungrovirus*), those of two unassigned *Caulimoviridae*, Blueberry fruit drop associated
157 virus (BFDaV, (Diaz-Lara and Martin, 2016)) and Rudbeckia flower distortion virus (RuFDV, (Lockhart
158 et al., 2017)), and those of endogenous caulimovirids from the tentative genera Orendovirus
159 (Geering et al., 2010) and Florendovirus (Geering et al., 2014). From this library of caulimovirid
160 genomes, we aligned the genomic regions containing the conserved protease, reverse transcriptase
161 and ribonuclease H1 domains to build a maximum likelihood phylogenetic tree (Figure 3).

162

163 This tree confirmed that the reconstructed genomes clade within the *Caulimoviridae*. In agreement
164 with previous studies (Geering et al., 2014), the tree revealed two sister clades (hereafter referred to
165 as clade A and B). Clade A comprised sequences from representatives of Xendovirus and Yendovirus
166 OTUs and from members of genera *Caulimovirus*, *Soymovirus*, *Rosadnavirus*, *Solendovirus*,
167 *Cavemovirus*, *Badnavirus*, *Tungrovirus* and Orendovirus, as well as from unassigned RuFDV and
168 BFDaV. Noteworthy, the two sequences reconstructed from the Xendovirus OTU appear to clade at

169 distant positions in the phylogenetic tree: the one from *Gossypium raimondii* (cotton) is most closely
170 related to the cluster encompassing sequences from genera *Cavemovirus* and *Solendovirus* whereas
171 the one reconstructed from *Fragaria vesca* (wild strawberry) is closer to BFDaV. This sequence from
172 *Fragaria vesca* was hence reclassified in an additional OTU named Zendovirus. The representative
173 sequence for Yendovirus, reconstructed from *Capsicum annuum* (bell pepper), is most closely related
174 to the clade comprising representatives of the genera *Badnavirus*, *Tungrovirus* and Orendovirus.

175
176 Clade B comprised sequences from representatives of the four gymnendovirus OTUs and those from
177 ferns and clubmoss, as well as sequences from genera Florendovirus and *Petuvirus*. Sequences from
178 Fernendovirus 1 & 2 clade together, the clubmoss sequence being collapsed in Fernendovirus 1
179 (Figure 3). *Petuvirus* clade is sister to Fernendovirus 2 though with a significant level of uncertainty
180 (bootstrap value=49%). Gymnendovirus 1 is sister to the Fernendo/*Petuvirus* clade whereas
181 Gymnendovirus 3 and 4 form a cluster that is sister to Florendovirus. Gymnendovirus 2 sequences
182 group in a clade that is sister to all other clade B viruses. Noteworthy, reconstructed genomes from
183 novel OTUs found in single dicotyledon species (*Petunia*-, *Vitis*-, and *Glycine*-endovirus) were
184 discarded from the phylogenetic reconstruction as they appeared to significantly weaken the
185 robustness of the tree. They could however be placed unambiguously in clade A (data not shown).

186

187 **ECRT distribution across seed plant genomes**

188 To address the distribution of caulimovirid EVEs in our collection of plant genomes, we determined
189 the most likely phylogenetic position within the reference *Caulimoviridae* phylogenetic tree proposed
190 above (Figure 3) for the 14,895 ECRTs that we collected from seed plant genomes using the pplacer
191 program (Matsen et al., 2010). For this, we extracted ECRT loci extending upstream and downstream
192 so as to retrieve potential sequences containing the contiguous fragment corresponding to the
193 protease, RT and ribonuclease H1 domains. Using more relaxed length criteria, we extracted a total
194 of 134 ECRT loci from the fern genomic data set that we also attempted to place on our reference
195 tree.

196

197 Applying this strategy, we were able to assign unambiguous phylogenetic position on specific OTUs
198 to a total of 13,834 ECRTs (Figure 4), the remaining ECRT loci being placed on inner nodes of the
199 reference tree. Overall, we observed striking differences between Caulimoviridae genera for both the
200 number of ECRT loci and the number of plant species in which they were found. For instance,
201 Florendovirus ECRT loci were the most abundant, amounting to an overall total of 5k copies and they
202 were also found in the highest number of host species (46 of the 62 seed plant species that were
203 screened). *Petuvirus* ECRT loci were also well represented, with an overall total of 1.9k copies found
204 in a total of 27/62 seed plant species, especially in dicots. Among the novel OTUs, ECRTs classified as
205 Yendovirus were found in the largest number of species, including monocots and dicots (Figure 4).

206

207 Most importantly, the detailed distribution of *Caulimoviridae* in plant genomes reveals striking
208 differences between lycopods, ferns, gymnosperms and angiosperms (Figure 4). No single OTU spans
209 several plant divisions on Figure 4 (which describes plant genomic contents) but Fernendovirus 1
210 sequences are found in both fern genomes and lycopod transcriptome. Fern genomes contain
211 exclusively ECRT loci that are classified as Fernendovirus 1 & 2. In corollary, Fernendovirus ECRTs are
212 found only in club moss and ferns. Gymnosperm genomes enclose exclusively ECRT loci that are
213 assigned to one of the four Gymnendovirus OTUs, all of which being undetected outside of

214 gymnosperms. Among gymnosperms, the three conifer genomes analyzed contain a mixture ECRTs
215 from the four Gymnendovirus genera. By contrast, only ECRT loci classified as Gymnendovirus 2 were
216 detected in *Ginkgo biloba* (*Ginkgoales*). Within angiosperms, we also observed a dichotomy for the
217 distribution of ECRTs between monocots and dicots. On one hand, Yendovirus, Badnavirus,
218 Orendovirus and Florendovirus ECRTs are common in monocots. On the other hand, Petuvirus,
219 Florendovirus, Xendovirus, Cavemovirus/Solendovirus and Yendovirus ECRTs are the most widely
220 distributed in dicots, Florendovirus and Yendovirus hence being remarkably well represented in both
221 dicots and monocots.

222

223 Discussion

224 Endogenous viral elements are considered relics of past infections, and an extrapolation of the
225 results from this study is that nearly every tracheophyte plant species in the world has at some point
226 in its evolutionary history been subject to infection by at least one, and sometimes five distinct viral
227 species/genera from the family *Caulimoviridae*. This finding attests to the tremendous adaptability of
228 the *Caulimoviridae*, surpassing any other groups of plant viruses. Members of the *Caulimoviridae*
229 have likely also had a large influence on plant evolution, either as pathogens or donors of novel
230 genetic material to the plant genome.

231

232 Our findings provide insights into the evolutionary history of the *Caulimoviridae*. Nine new OTUs
233 were detected, each of which likely representing several virus genera. In addition, we detected
234 sequences defining three additional OTUs that were initially detected in only one plant species (or
235 genus in the case of *Petunia*) (Figure 1). Considering that we have discovered nine putative novel
236 genera in the family *Caulimoviridae* by screening over 60 genomes from a variety of land plants,
237 compared to the eight current genera in this family, one can reasonably assume that the systematic
238 search for caulimovirid EVEs in the incoming flow of plant genomic resources will further increase the
239 amount of viral species in this family, and probably the number of OTUs in the *Caulimoviridae*.

240

241 A defining moment in the evolution of the *Caulimoviridae* appears to be the development of
242 vasculature in plants. The presence of a 30K movement protein is an important feature of the
243 *Caulimoviridae* that distinguishes it from the *Metaviridae*, and this protein is crucial for the formation
244 of systemic infection by allowing intercellular trafficking of macromolecules through increasing the
245 size exclusion limit of plasmodesmata (Link and Sonnewald, 2016). Although algae contain
246 plasmodesmata, which superficially resemble those of higher plants, they are not homologous and
247 their molecular structure is different from that of higher plants (Brunkard and Zambryski, 2017).
248 While the acquisition of a 30K movement protein would have provided a selective advantage for
249 ancestral caulimovirids to colonize the tracheophytes, it would not have facilitated infection of more
250 primitive plant forms.

251

252 In light of the results, one of the most surprising findings was the absence of ECRTs in a select
253 number of plant species such as *Arabidopsis thaliana*. Given that close relatives of *A. thaliana*, such
254 as *A. lyrata*, contain ECRTs, it is unlikely that *A. thaliana* has avoided infection either through chance
255 or because of disease resistance. One of the special traits of *A. thaliana* is its very small genome size,
256 a reason it has developed as a model plant species. Comparisons of *A. thaliana* with large-genome
257 plant species such as *Nicotiana tabacum* and *Hordeum vulgare* suggest that there are marked
258 differences in double-stranded break repair (DSB) mechanisms (Orel and Puchta, 2003) (Vu et al.,

259 2017). The frequency and size of DNA insertions after DSB is much higher for *H. vulgare* compared to
260 *A. thaliana*, and conversely, the size of deletions much higher for *A. thaliana*. These intrinsic
261 differences in DSB between plant species have likely acted against the accumulation of EVEs in *A.*
262 *thaliana*.

263

264 The correlation between plant genome size and the number of ECRTs (Figure 2A) may also suggest
265 that extensive heterochromatic regions as found in large genomes are relatively permissive to the
266 retention of *Caulimoviridae* insertions compared to gene-rich regions. In this regard, Florendovirus
267 EVEs are so widespread in dicotyledon species that their absence from the medium sized genomes of
268 *Medicago truncatula* (412 Mbp) and *Cannabis sativa* (585 Mbp) is remarkable and could reflect
269 acquired resistance in these species. In contrast, peculiar dynamics of *Caulimoviridae* integration
270 could explain the relatively high density of ECRTs observed in the sweet orange and castor bean
271 genomes. Finally, the absence of ECRT in the genome of the monocotyledon plant *Zostera marina* is
272 not surprising considering its marine lifestyle (Olsen et al., 2016) and it stresses that the return to the
273 sea undergone by some flowering plants also provided an escape from terrestrial viruses.

274

275 We can assume that the extinction of viral genera is common over long evolutionary scales, due to
276 the extinction of vectors or the development of plant resistance. Therefore, one can expect that only
277 a fraction of ancestral *Caulimoviridae* is represented in their modern descendants, whether
278 endogenous or exogenous. Therefore our results need to be interpreted with the consideration that,
279 most probably, many unknown *Caulimoviridae* genera are lacking from our phylogeny. Moreover,
280 incomplete lineage sorting can cause two sequences separated by a whole world of
281 extinct/unavailable sequences to appear most closely related in phylogenetic reconstructions. We
282 also consider that the most parsimonious path to explain the spread of viruses within host taxonomy
283 is vertical transmission. Vertical transmission is well supported by a co-evolutionary study of
284 Florendovirus EVEs and their host species (Geering et al., 2014) and it is probably also the leading
285 route followed by retroviruses along with their host species (Hayward et al., 2015). Following a co-
286 evolutionary scenario by pure vertical transmission, a virtually complete phylogeny of *Caulimoviridae*
287 genera should mirror the one of host species. If the last common host associated with two different
288 genera, then the vertical transmission of each ancestral genus would lead to two paralog clusters,
289 each mirroring host evolution, just as ancestrally duplicated genes would show in modern species.

290

291 Indeed, we can note a relatively deep cluster in clade B in which *Caulimoviridae* evolution to a large
292 extent mirrors host evolution over major divisions of land plants (Figure 5). This cluster is hereafter
293 referred to as modern mirror (mm) cluster. Within the mm cluster, the *Caulimoviridae* sequence
294 isolated from clubmoss is most closely related to ECRT from ferns and is included in Fernendovirus 1
295 OTU. *Petuvirus* is sister to both Fernendovirus OTUs but with significant uncertainty. A cluster
296 containing sequences from angiosperms and gymnosperms branches at the base of this group. The
297 finding that the phylogeny of some *Caulimoviridae* mirrors the evolution of plant species prompted
298 us to further elaborate on the evolutionary history of the *Caulimoviridae* based principally on vertical
299 transmission in order to interpret the observed *Caulimoviridae*-plant associations.

300

301 Reconciling our data with a vertical transmission-based co-evolutionary scenario, the mm cluster
302 would be unique in that its last common ancestor would be represented by modern descendants
303 that associate with species from the four plant divisions (angiosperms, gymnosperms, ferns, and

304 clubmoss). In this cluster, the phylogenetic relationships between viruses and between plants can be
305 interpreted by coevolution through vertical transmission while introducing very few viral speciation
306 events and gaps filling due to extinct or non-sampled sequences. As vertical transmission goes
307 forward, ancient *Caulimoviridae* would have associated with the ancestor of modern clubmoss
308 species. The position of the genus that associates with modern clubmoss in the mm cluster, *i.e.*
309 Fernendovirus 1, supports this hypothesis.

310
311 Deeper in the evolutionary history of the *Caulimoviridae*, our working scenario would involve the
312 existence of a last common ancestor (LCA) of *Caulimoviridae* at latest during the emergence of
313 clubmoss, *i.e.* towards the end of the Silurian era 420 MYA (Hedges et al., 2006). Before the
314 emergence of ferns about 380 MYA, the speciation of *Caulimoviridae* LCA would have evolved into
315 the ancestors of clade A and B and both would have continued vertical transmission with their host.
316 The absence of ECRTs from modern descendants in the (non-mm) clusters could then be explained
317 mainly by their relatively ancient death and/or by limited sampling (Figure 5).

318 We consider that an alternative scenario that would involve a significant number of host swaps
319 between plant divisions is counter intuitive considering the current data, because several of these
320 swaps would actually overlap with plant evolutionary history, as exemplified in the mm cluster.
321 Therefore, we currently favor at the earliest Silurian origin of the *Caulimoviridae* followed by viral
322 speciation and then principally by vertical transmission from the emergence of ferns to later
323 bifurcations in plant evolution.

324
325

326 **Supplementary material**

327 Supplementary file 1: reconstructed ancestral sequences of members of the *Caulimoviridae* from
328 novel OTUs (fasta format).

329
330

331 **Figure legends**

332 Figure 1: Augmented diversity of the *Caulimoviridae*. Core of a phylogenetic network constructed
333 using an alignment of amino acid reverse transcriptase (RT) sequences from reference genera,
334 representative endogenous caulimovirid RTs (ECRTs) and Ty3/Gypsy LTR retrotransposons. The full
335 network is available in Supplementary Figure 1. This representation allows determining 17
336 *Caulimoviridae* OTUs. OTU names have dashed lime green outline when they include no known
337 reference genera (referred to as novel OTUs). Each fill color corresponds to a different OTU except
338 for OTUs comprising only a representative ECRT sequence that are colored with dark grey and named
339 after the only host plant genome they were detected in at this stage (Petunia-, Vitis-, and Glycine-
340 virus). * RT clustering at 55% identity groups Cavemovirus and Solendovirus into a single OTU (OTU
341 8). ** Sequences grouped in the Xendovirus OTU appeared to be paraphyletic after phylogenetic
342 reconstruction (see Figure 3).

343

344 Figure 2: Highly variable ECRT numbers and density across plants. (A) Number of ECRTs found in each
345 plant genome as function of Log₁₀ genome size expressed in megabases (assembly gaps excluded).
346 Logarithmic trendline indicates moderate correlation between the number of ECRT and genome size
347 ($R^2=0.544$). (B) Density of ECRTs per megabase in each plant genome as function of Log₁₀ genome

348 size expressed in megabases (assembly gaps excluded). In (A) and (B), arrows indicate a sample of
349 outlier dots and the corresponding plant species name.

350

351 Figure 3: Phylogeny of the *Caulimoviridae*. Phylogenetic tree obtained by maximum likelihood search
352 from a multiple sequence alignment of the genomic regions containing protease, reverse
353 transcriptase and ribonuclease H1 domains from known (black) and novel (red) *Caulimoviridae*
354 genera. The sequences from Gypsy and Ty3 LTR retrotransposons are used as outgroups. Bootstrap
355 support values below 50% are not shown. Sequences from members of the novel genera are
356 available in supplementary data. Closely related sequences were collapsed into branches. The
357 sequences contained in each branch are as follows. Orendovirus: *Aegilops tauschii* virus (AtV),
358 *Brachypodium distachyon* virus (BdV); *Tungrovirus*: *Rice tungro bacilliform virus* (RTBV), *Rice tungro*
359 *bacilliform virus isolate west Bengal* (RTBV); *Badnavirus*: *Commelina yellow mottle virus* (ComYMV),
360 *Banana streak OL virus* (BSOLV); *Yendovirus*: *Capiscum annuum virus*; *Zendovirus*: *Fragaria vesca*
361 *virus*; *Blueberry*: *Blueberry fruit drop associated virus* (BFDaV); *Caulimovirus*: *Cauliflower mosaic*
362 *virus* (CaMV), *Figwort mosaic virus* (FMV); *Rudbeckia*: *Rudbeckia flower distortion virus* (RuFDV);
363 *Soymovirus*: *Soybean chlorotic mottle virus* (SoyCaulimoviridae), *Peanut chlorotic streak virus* (PCSV);
364 *Solendovirus*: *Sweet potato vein clearing virus* (SPVCV), *Tobacco vein clearing virus* (TVCV);
365 *Cavemovirus*: *Cassava vein mosaic virus* (CsVMV), *Sweet potato collusive virus* (SPCV); *Petuvirus*:
366 *Petunia vein clearing virus* (PVCV); *Rosadnavirus*: *Rose yellow vein virus* (RYVV); *Florendovirus*:
367 *Fragaria vesca virus* (FvesV), *Mimulus guttatus virus* (MgutV); *Gymnendovirus 1*: *Pinus taeda*
368 *Gymnendovirus 1*, *Picea glauca Gymnendovirus 1*; *Gymnendovirus 2*: *Pinus taeda Gymnendovirus 2*,
369 *Picea glauca Gymnendovirus 2*, *Ginkgo biloba Gymnendovirus 2*; *Gymnendovirus 3*: *Pinus taeda*
370 *Gymnendovirus 3*; *Gymnendovirus 4*: *Pinus taeda Gymnendovirus 4*, *Picea glauca Gymnendovirus 4*;
371 *Fernendovirus 1*: *Cystopteris protrusa Fernendovirus 1 contig 1*, and the transcript scaffolds BEGM-
372 2004510 from *Botrypus virginianus*, NOKI-2097008 from *Lindsaea linearis*, and ENQF-2084799 from
373 *Lycopodium annotinum*; *Fernendovirus 2*: *Dipteris conjugata Fernendovirus 2 Contigs 2, 4 and 1319*.

374

375 Figure 4: Distribution of endogenous *Caulimoviridae* in Euphyllophyte. The left tree represents a
376 cladogram of Euphyllophyte species investigated in this study. The name of major branches and
377 nodes is indicated. The top tree represents the topology of the phylogenetic tree obtained in Figure
378 3. At the intersection of these two trees, color code indicates the number of ECRT loci classified into
379 each *Caulimoviridae* genus for each plant species. Abbreviations of *Caulimoviridae* genera are as
380 follows: Pe (Petuvirus), Gy1 (Gymnendovirus 1), Gy2 (Gymnendovirus 2), Gy3 (Gymnendovirus 3),
381 Gy4 (Gymnendovirus 4), Fe1 (Fernendovirus 1), Fe2 (Fernendovirus 2), Flo (Florendovirus), Soy
382 (Soymovirus), Rud (Rudbeckia flower distortion virus), Cau (Caulimovirus), Blu (Blueberry fruit drop
383 associated virus), Zen (Zendovirus), Xen (Xendovirus), Yen (Yendovirus), CaS (Cavemovirus
384 +Solendovirus), Ros (Rosadnavirus), Bad (Badnavirus), Tun (Tungrovirus), Ore (Orendovirus).

385

386 Figure 5: Working scenario of *Caulimoviridae* deep evolution. The left tree is the same as in Figure 3
387 where the deepest *Caulimoviridae* node was annotated as LCA (last common ancestor) and its two
388 daughter nodes were annotated Clade A and Clade B. The modern mirror (mm) cluster is delimited
389 by a green rectangle. Well supported branches within the mm cluster have been casted with dashed
390 blue lines onto a cladogram, on the right, that recapitulates the relationships between major
391 trachepohyte divisions (branches are annotated following the date of emergence of the different
392 plant divisions in million years ago (MYA).

393

394 Supplementary Figure 1: Overview of the phylogenetic network used to build Figure 1.

395

396 Supplementary Figure 2: ECRT ORFs collected from ferns cluster as two novel OTUs. Representative
397 sequences identified in fern genomes were appended to the collection of sequences represented in
398 Figure 1. The resulting library has been re-aligned with MUSCLE and phylogenetic network was built
399 using SplitsTree. The branches containing fern sequences have been empirically grouped into two
400 novel OTUs.

401

402

403 **Methods**

404 **Discovery and clustering of novel Caulimoviridae OTUs**

405 We built a library containing an assortment of amino acid (aa) sequences from 54 RT domains
406 including four from *Retroviridae*, 6 from Ty3/Gypsy LTR retrotransposons, 41 from 8 different known
407 Caulimoviridae genera (*Florendovirus*, *Caulimovirus*, *Tungrovirus*, *Cavemovirus*, *Solendovirus*,
408 *Badnavirus*, *Soymovirus*, and *Petuvirus*), 2 from *Picea glauca* identified ahead as belonging to new
409 Caulimoviridae genera, and the one from the DIRS-1 element. We compared this library to a
410 collection of 72 genome assemblies from Viridiplantae species (listed in Supplementary Table 1)
411 using tBLASTn with default parameters (except $-e=1e-5$). The hit genomic loci were merged when
412 overlapping and their coordinates were extended 120 bases upstream and downstream. Extended
413 hit loci were translated and the protein sequences of length ≥ 200 aa were compared to the initial RT
414 library using BLASTp with default parameters (except $-e=1e-5$). Queries with best alignment score
415 against Caulimoviridae over at least 170 residues were selected for further analysis. For each plant
416 species, the selected set of RT aa sequences have been clustered following sequence similarity using
417 the UCLUST program (Edgar, 2010) with identity threshold set at 80%. The longest sequence from
418 each resulting cluster was considered as the representative sequence and it was appended to the
419 initial RT library. To detect potential false positives, each set of sequences (each consisting of the
420 initial RT library and cluster representatives from one species) was aligned using MUSCLE followed by
421 filtering of lower fit sequences using two rounds of trimAl v1.2 (Capella-Gutierrez et al., 2009) to
422 remove poorly aligned sequences ($-\text{resoverlap } 0.75$ $-\text{seqoverlap } 50$) separated by one round to
423 remove gaps from the alignment ($-\text{gt } 0.5$). The representative sequences from each plant species that
424 passed this selection have then been combined into a single file and appended to the initial RT library
425 to be clustered with UCLUST using an identity threshold of 55%. At this level of similarity, aa RT
426 sequences from every Caulimoviridae genera fall into distinct clusters except those from
427 *Cavemovirus* and *Solendovirus* that cluster together. Starting with the first cluster, one or more
428 sequences presenting high quality alignment and containing several conserved residues as
429 determined contextually for each cluster were then manually selected to be representative of the
430 diversity observed within each cluster. The following clusters were processed similarly while keeping
431 the representative sequences selected from previously processed clusters. Clusters containing ECRT
432 sequences from only one plant species were analyzed only when they contained at least 3
433 sequences. After processing each cluster individually, a total of 56 ECRT sequences detected here and
434 20 RT from known genera have been selected for their remarkable divergence. Together with 4 RT
435 sequences from Ty3/Gypsy LTR retrotransposons, these combined sequences (hereafter referred to
436 as “diverse library”) were aligned with the GUIDANCE2 (Sela et al., 2015) program using MAFFT
437 (Katoh and Standley, 2013) to generate bootstrap supported MSA and to remove columns (--

438 colCutoff) with confidence score below 0.95 (16/244 columns removed in the RT sequence from
439 Caulimovirus CaMV). The resulting MSA was then used to build the phylogenetic network shown in
440 Figure 1 and Supplementary Figure 1 with SplitsTree4 (Huson and Bryant, 2006) applying the
441 NeighborNet method with uncorrected P distance model and 1,000 bootstrap tests. Manual analysis
442 of this network enabled the empirical discrimination of 17 distinct OTUs among Caulimoviridae
443 sequences.

444 Because initial search allowed discovering several novel OTUs, we repeated ECRT mining in plant
445 genomes using the diverse library as query. This second search is also designed to be more sensitive
446 as it takes into account DNA sequences instead of uninterrupted ORFs. The workflow is identical to
447 the one employed for the initial search until obtaining the set of extended hit loci. These were
448 directly compared to the diverse library using BLASTx with default parameters (except $-e=1e-5$).
449 Queries with best alignment score against any Caulimoviridae with an alignment length above 80% of
450 subject length (set generically to 576 bp considering an average size of RT domains of 240 aa) were
451 selected for phylogenetic placement.

452

453 **Phylogenetic analysis**

454 Fragments of virus sequence were assembled using CodonCode aligner 6.0.2 using default settings or
455 using VECTOR NTI Advance 10.3.1 (Invitrogen) operated using default settings, except that the values
456 for maximum clearance for error rate and maximum gap length were increased to 500 and 200,
457 respectively.

458 Phylogenetic reconstruction was performed using the contiguous nucleotide sequences
459 corresponding to the protease, reverse transcriptase and ribonuclease H domains. Whole sequences
460 from Caulimoviridae genera representatives and Ty3 and Gypsy LTR retrotransposons were first
461 aligned with global method using MAFFT v7.3 (Katoh and Standley, 2013). The core genomes was
462 extracted and re-aligned by local method using MAFFT. The resulting alignment was tested for
463 different evolutionary models with pmodeltest v1.4 (from ETE 3 package (Huerta-Cepas et al., 2016))
464 which inferred the GTRGAMMA model. Phylogenetic inference with maximum likelihood was then
465 performed using RaxML v8.2 (Stamatakis, 2014) under the predicted model with 500 ML bootstrap
466 replicates.

467 The resulting tree was then used as a reference to classify the ECRT loci mined from plant genomes.
468 We first added query sequences from each plant species separately to the reference alignment and
469 aligned each library using Mafft v7.3 (with options `--addfragment`, `--keeplength` and `by reordering`).
470 We then tested the most likely placement of each ECRT sequence on to the reference tree using
471 pplacer v1.1 alpha19 (Matsen et al., 2010) with the option (`--keep-at-most 1`) with allows to keep one
472 placement for each query sequence. The python package Taxit was used to construct a reference
473 package which we used to run pplacer.

474

475

476 **References**

- 477 AIEWSAKUN, P. & KATZOURAKIS, A. (2015) Endogenous viruses: Connecting recent and ancient viral
478 evolution. *Virology*, 479-480, 26-37.
- 479 AIEWSAKUN, P. & KATZOURAKIS, A. (2017) Marine origin of retroviruses in the early Palaeozoic Era.
480 *Nat Commun*, 8, 13954.
- 481 BEJARANO, E. R., KHASHOGGI, A., WITTY, M. & LICHTENSTEIN, C. (1996) Integration of multiple
482 repeats of geminiviral DNA into the nuclear genome of tobacco during evolution. *Proc Natl*
483 *Acad Sci U S A*, 93, 759-64.

- 484 BRUNKARD, J. O. & ZAMBRYSKI, P. C. (2017) Plasmodesmata enable multicellularity: new insights into
485 their evolution, biogenesis, and functions in development and immunity. *Curr Opin Plant Biol*,
486 35, 76-83.
- 487 CAPELLA-GUTIERREZ, S., SILLA-MARTINEZ, J. M. & GABALDON, T. (2009) trimAl: a tool for automated
488 alignment trimming in large-scale phylogenetic analyses. *Bioinformatics*, 25, 1972-3.
- 489 DIAZ-LARA, A. & MARTIN, R. R. (2016) Blueberry fruit drop-associated virus: A New Member of the
490 Family Caulimoviridae Isolated From Blueberry Exhibiting Fruit-Drop Symptoms. *The*
491 *American Phytopathological Society*, 100, 2211-2214.
- 492 EDGAR, R. C. (2010) Search and clustering orders of magnitude faster than BLAST. *Bioinformatics*, 26,
493 2460-1.
- 494 GEERING, A. D., MAUMUS, F., COPETTI, D., CHOISNE, N., ZWICKL, D. J., ZYTNIICKI, M., MCTAGGART, A.
495 R., SCALABRIN, S., VEZZULLI, S., WING, R. A., QUESNEVILLE, H. & TEYCHENEY, P. Y. (2014)
496 Endogenous florendoviruses are major components of plant genomes and hallmarks of virus
497 evolution. *Nat Commun*, 5, 5269.
- 498 GEERING, A. D., SCHARASCHKIN, T. & TEYCHENEY, P. Y. (2010) The classification and nomenclature of
499 endogenous viruses of the family Caulimoviridae. *Arch Virol*, 155, 123-31.
- 500 HANSEN, C. & HESLOP-HARRISON, J. S. (2004) Sequences and phylogenies of plant pararetroviruses,
501 viruses, and transposable elements. *Advances in Botanical Research*, 41, 165-193.
- 502 HAYWARD, A., CORNWALLIS, C. K. & JERN, P. (2015) Pan-vertebrate comparative genomics unmasks
503 retrovirus macroevolution. *Proc Natl Acad Sci U S A*, 112, 464-9.
- 504 HEDGES, S. B., DUDLEY, J. & KUMAR, S. (2006) TimeTree: a public knowledge-base of divergence
505 times among organisms. *Bioinformatics*, 22, 2971-2.
- 506 HUERTA-CEPAS, J., SERRA, F. & BORK, P. (2016) ETE 3: Reconstruction, Analysis, and Visualization of
507 Phylogenomic Data. *Mol Biol Evol*, 33, 1635-8.
- 508 HUSON, D. H. & BRYANT, D. (2006) Application of phylogenetic networks in evolutionary studies. *Mol*
509 *Biol Evol*, 23, 254-67.
- 510 KATOH, K. & STANDLEY, D. M. (2013) MAFFT multiple sequence alignment software version 7:
511 improvements in performance and usability. *Mol Biol Evol*, 30, 772-80.
- 512 LINK, K. & SONNEWALD, U. (2016) Interaction of Movement Proteins with Host Factors, Mechanism
513 of Viral Host Cell Manipulation and Influence of MPs on Plant Growth and Development. IN
514 KLEINOW, T. (Ed.) *Plant-Virus Interactions: Molecular Biology, Intra- and Intercellular*
515 *Transport*. Cham, Springer International Publishing.
- 516 LOCKHART, B., MOLLOV, D., OLSZEWSKI, N. & GOLDSMITH, N. (2017) Identification, transmission and
517 genomic characterization of a new member of the family Caulimoviridae causing a flower
518 distortion disease of *Rudbeckia hirta*. *Virus Res*, In Press, Corrected Proof.
- 519 MATASCI, N., HUNG, L. H., YAN, Z., CARPENTER, E. J., WICKETT, N. J., MIRARAB, S., NGUYEN, N.,
520 WARNOW, T., AYYAMPALAYAM, S., BARKER, M., BURLEIGH, J. G., GITZENDANNER, M. A.,
521 WAFULA, E., DER, J. P., DEPAMPHILIS, C. W., ROURE, B., PHILIPPE, H., RUHFEL, B. R., MILES, N.
522 W., GRAHAM, S. W., MATHEWS, S., SUREK, B., MELKONIAN, M., SOLTIS, D. E., SOLTIS, P. S.,
523 ROTHFELS, C., POKORNY, L., SHAW, J. A., DEGIRONIMO, L., STEVENSON, D. W., VILLARREAL, J.
524 C., CHEN, T., KUTCHAN, T. M., ROLF, M., BAUCOM, R. S., DEYHOLOS, M. K., SAMUDRALA, R.,
525 TIAN, Z., WU, X., SUN, X., ZHANG, Y., WANG, J., LEEBENS-MACK, J. & WONG, G. K. (2014) Data
526 access for the 1,000 Plants (1KP) project. *Gigascience*, 3, 17.
- 527 MATSEN, F. A., KODNER, R. B. & ARMBRUST, E. V. (2010) pplacer: linear time maximum-likelihood
528 and Bayesian phylogenetic placement of sequences onto a fixed reference tree. *BMC*
529 *Bioinformatics*, 11, 538.
- 530 MUSHEGIAN, A. R. & ELENA, S. F. (2015) Evolution of plant virus movement proteins from the 30K
531 superfamily and of their homologs integrated in plant genomes. *Virology*, 476, 304-15.
- 532 OLSEN, J. L., ROUZE, P., VERHELST, B., LIN, Y. C., BAYER, T., COLLEN, J., DATTOLO, E., DE PAOLI, E.,
533 DITTAMI, S., MAUMUS, F., MICHEL, G., KERSTING, A., LAURITANO, C., LOHAUS, R., TOPEL, M.,
534 TONON, T., VANNESTE, K., AMIREBRAHIMI, M., BRAKEL, J., BOSTROM, C., CHOVIATIA, M.,
535 GRIMWOOD, J., JENKINS, J. W., JUETERBOCK, A., MRAZ, A., STAM, W. T., TICE, H.,

- 536 BORNBERG-BAUER, E., GREEN, P. J., PEARSON, G. A., PROCACCINI, G., DUARTE, C. M.,
537 SCHMUTZ, J., REUSCH, T. B. & VAN DE PEER, Y. (2016) The genome of the seagrass *Zostera*
538 *marina* reveals angiosperm adaptation to the sea. *Nature*, 530, 331-5.
- 539 OREL, N. & PUCHTA, H. (2003) Differences in the processing of DNA ends in *Arabidopsis thaliana* and
540 tobacco: possible implications for genome evolution. *Plant Mol Biol*, 51, 523-31.
- 541 ROOSSINCK, M. J. (2016) Deep sequencing for discovery and evolutionary analysis of plant viruses.
542 *Virus Res*.
- 543 SELA, I., ASHKENAZY, H., KATOH, K. & PUPKO, T. (2015) GUIDANCE2: accurate detection of unreliable
544 alignment regions accounting for the uncertainty of multiple parameters. *Nucleic Acids Res*,
545 43, W7-14.
- 546 STAMATAKIS, A. (2014) RAxML version 8: a tool for phylogenetic analysis and post-analysis of large
547 phylogenies. *Bioinformatics*, 30, 1312-1313.
- 548 TEYCHENEY, P. Y. & GEERING, A. D. (2011) Endogenous viral sequences in plant genomes. *Recent*
549 *advances in plant virology*. Norfolk, Caister Academic Press.
- 550 VU, G. T. H., CAO, H. X., REISS, B. & SCHUBERT, I. (2017) Deletion-bias in DNA double-strand break
551 repair differentially contributes to plant genome shrinkage. *New Phytol*, 214, 1712-1721.
- 552 WICKETT, N. J., MIRARAB, S., NGUYEN, N., WARNOW, T., CARPENTER, E., MATASCI, N.,
553 AYYAMPALAYAM, S., BARKER, M. S., BURLEIGH, J. G., GITZENDANNER, M. A., RUHFEL, B. R.,
554 WAFULA, E., DER, J. P., GRAHAM, S. W., MATHEWS, S., MELKONIAN, M., SOLTIS, D. E., SOLTIS,
555 P. S., MILES, N. W., ROTHFELS, C. J., POKORNY, L., SHAW, A. J., DEGIRONIMO, L., STEVENSON,
556 D. W., SUREK, B., VILLARREAL, J. C., ROURE, B., PHILIPPE, H., DEPAMPHILIS, C. W., CHEN, T.,
557 DEYHOLOS, M. K., BAUCOM, R. S., KUTCHAN, T. M., AUGUSTIN, M. M., WANG, J., ZHANG, Y.,
558 TIAN, Z., YAN, Z., WU, X., SUN, X., WONG, G. K. & LEEBENS-MACK, J. (2014)
559 Phylotranscriptomic analysis of the origin and early diversification of land plants. *Proc Natl*
560 *Acad Sci U S A*, 111, E4859-68.
- 561 WOLF, P. G., SESSA, E. B., MARCHANT, D. B., LI, F. W., ROTHFELS, C. J., SIGEL, E. M., GITZENDANNER,
562 M. A., VISGER, C. J., BANKS, J. A., SOLTIS, D. E., SOLTIS, P. S., PRYER, K. M. & DER, J. P. (2015)
563 An Exploration into Fern Genome Space. *Genome Biol Evol*, 7, 2533-44.
- 564 XIONG, Y. & EICKBUSH, T. H. (1990) Origin and evolution of retroelements based upon their reverse
565 transcriptase sequences. *EMBO J*, 9, 3353-62.
- 566
567

Figures

Figure 1

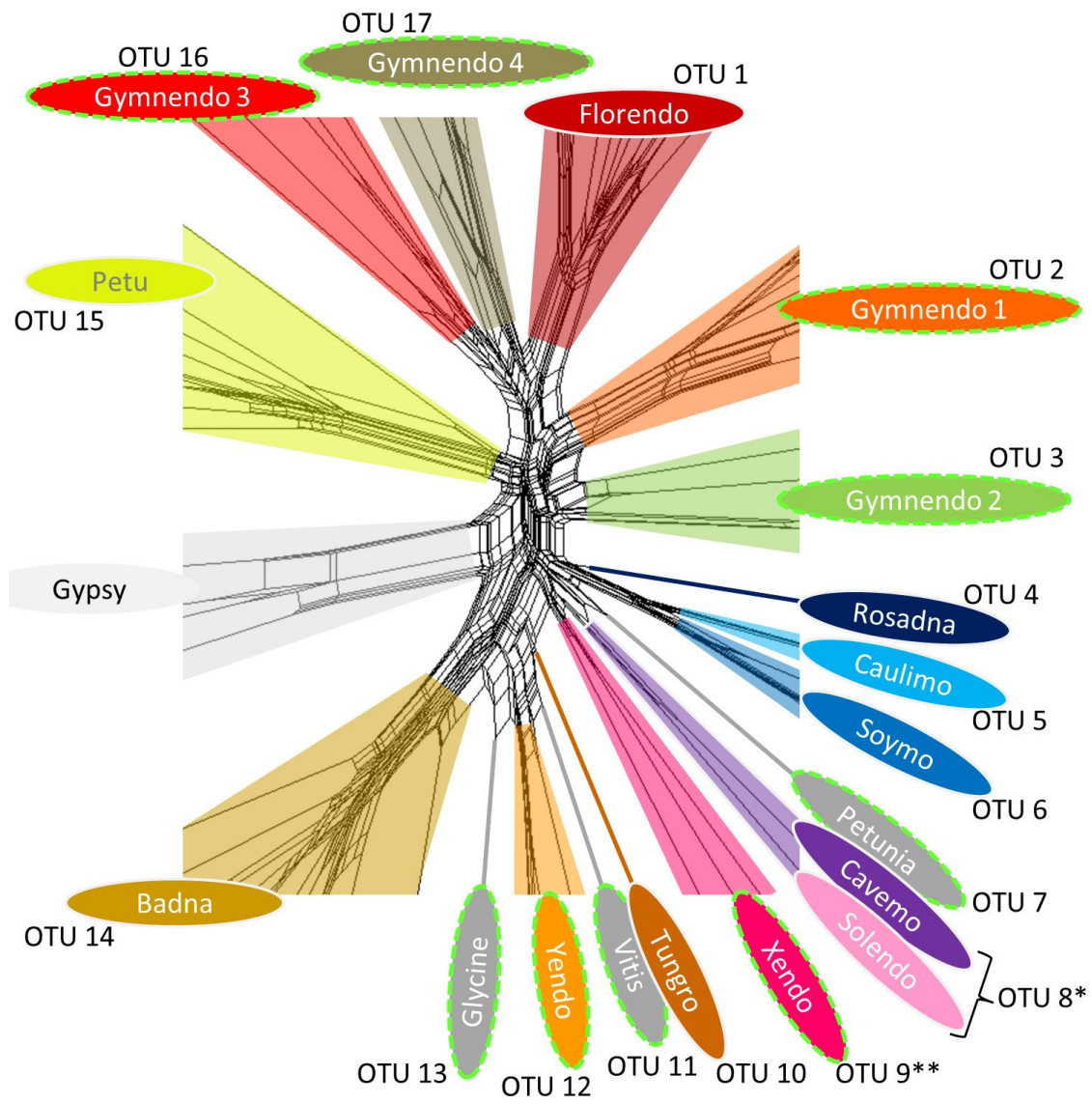


Figure 2

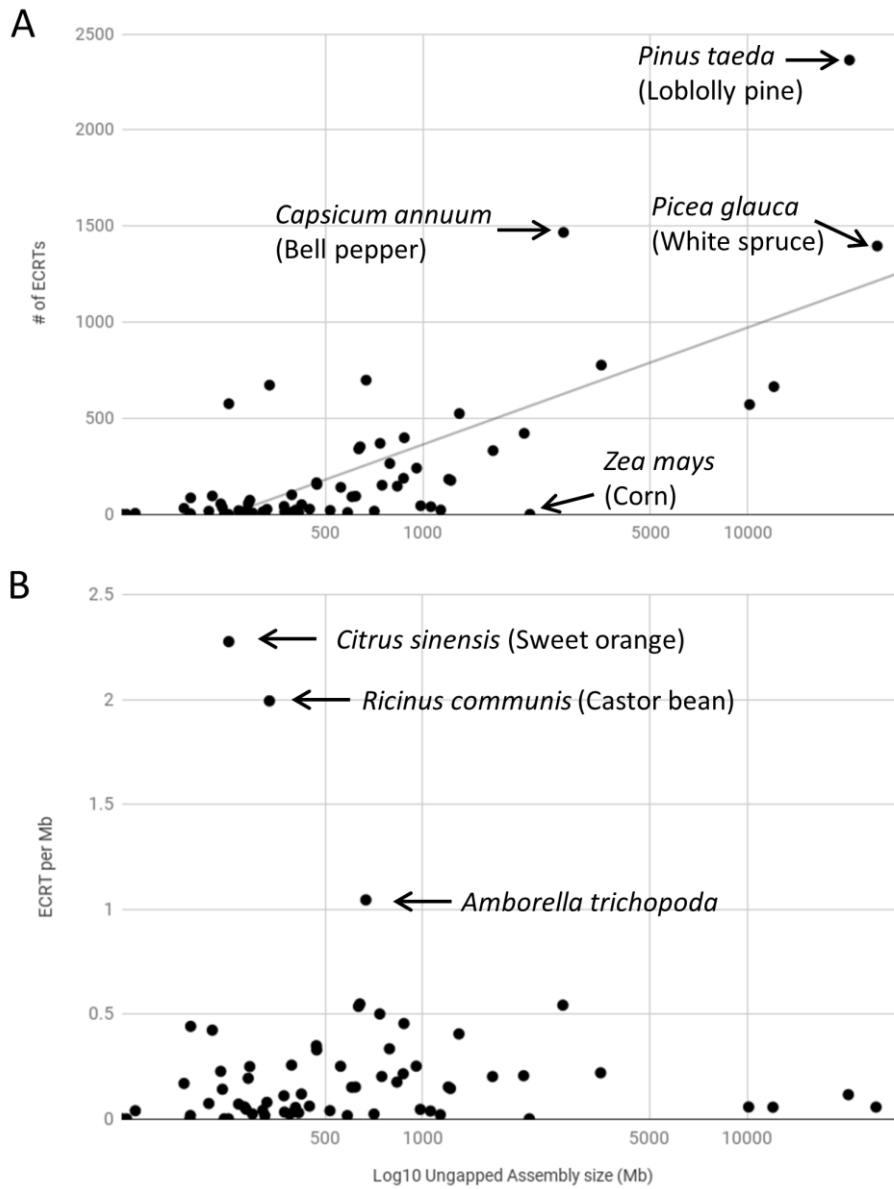


Figure 4

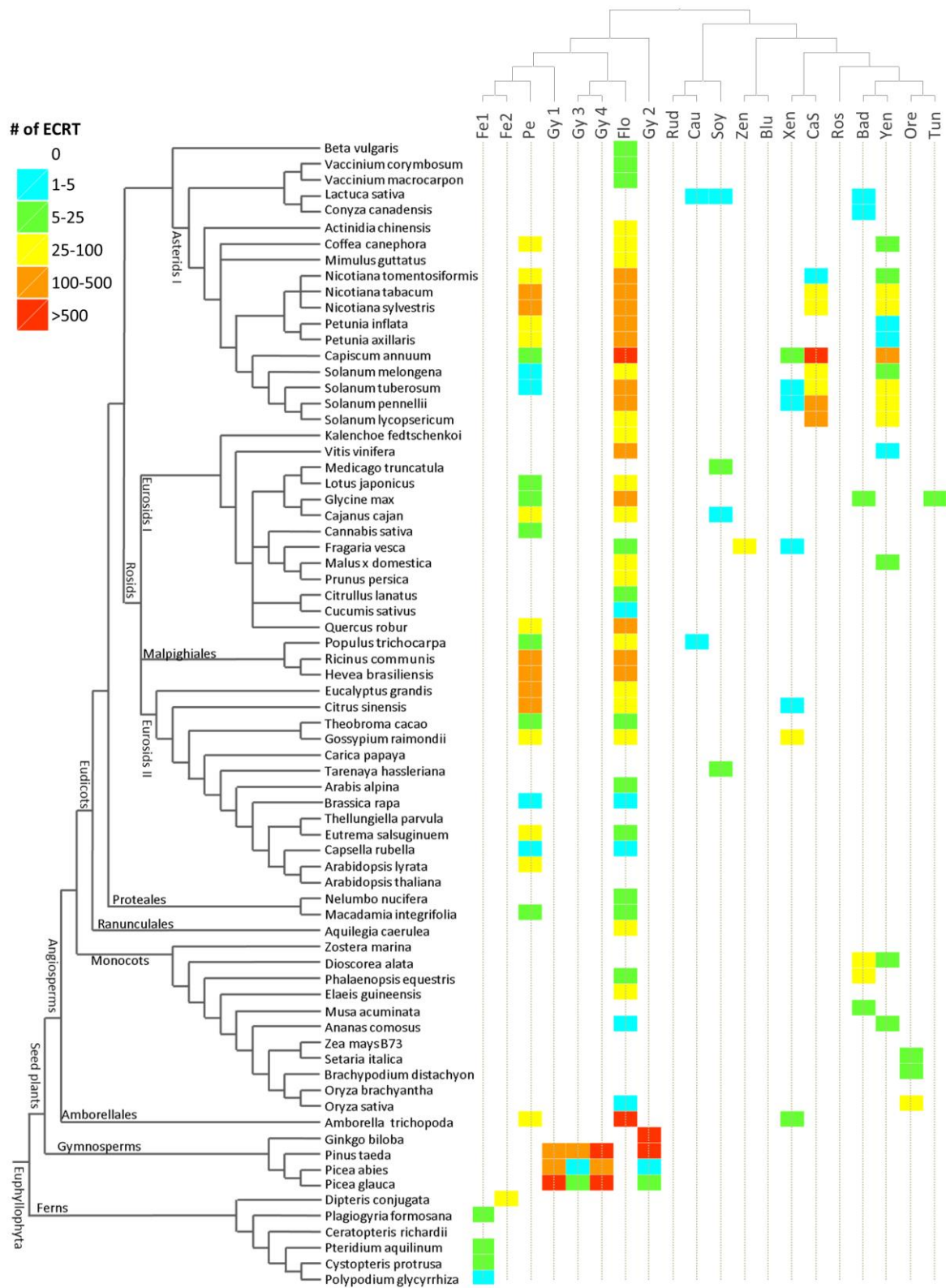
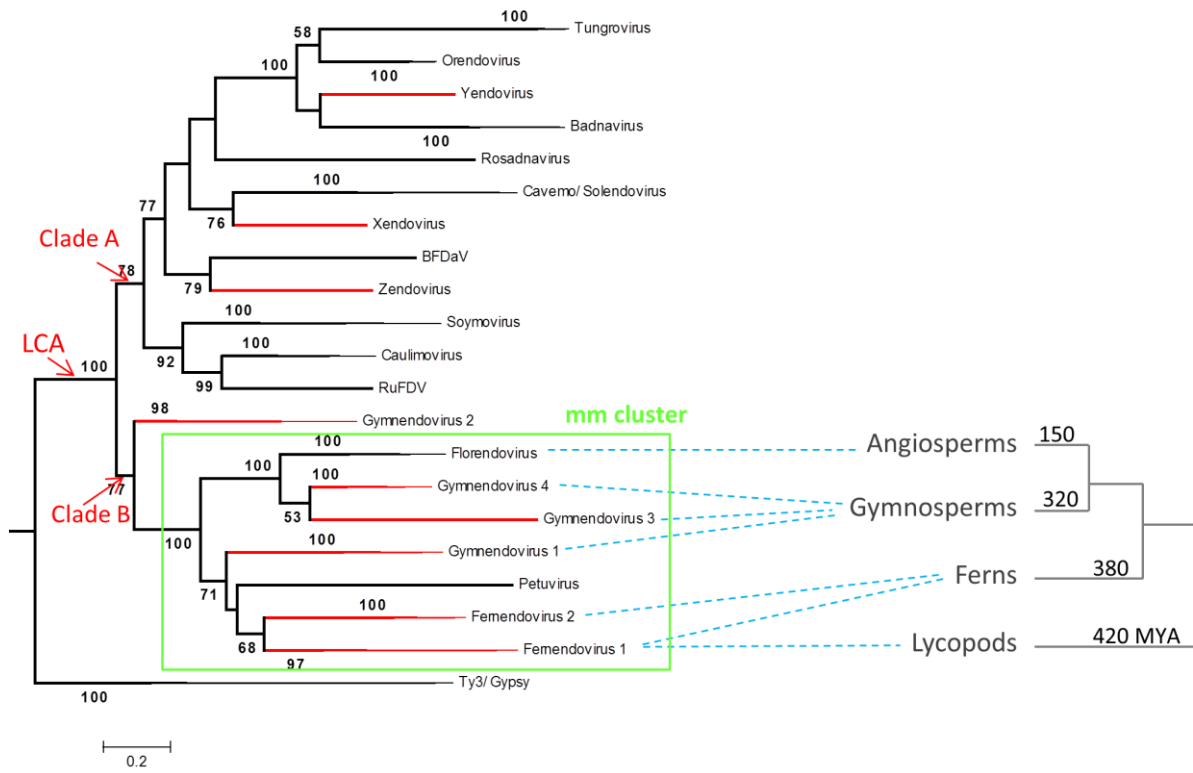


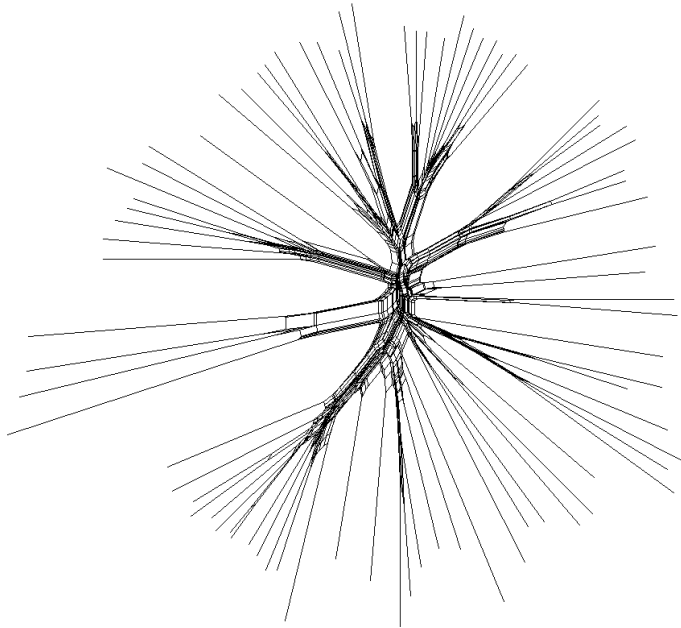
Figure 5



Supplementary figures

Supplementary figure 1

0.1



Supplementary figure 2

